

UC Berkeley

UC Berkeley Previously Published Works

Title

Windthrow characteristics and their regional association with rainfall, soil, and surface elevation in the Amazon

Permalink

<https://escholarship.org/uc/item/1kf448qf>

Journal

Environmental Research Letters, 18(1)

ISSN

1748-9318

Authors

Negron-Juarez, Robinson

Magnabosco-Marra, Daniel

Feng, Yanlei

et al.

Publication Date

2023

DOI

10.1088/1748-9326/acaf10

Copyright Information

This work is made available under the terms of a Creative Commons Attribution License, available at <https://creativecommons.org/licenses/by/4.0/>

Peer reviewed

LETTER • OPEN ACCESS

Windthrow characteristics and their regional association with rainfall, soil, and surface elevation in the Amazon

To cite this article: Robinson Negrón-Juárez *et al* 2023 *Environ. Res. Lett.* **18** 014030

View the [article online](#) for updates and enhancements.

You may also like

- [Quantifying long-term changes in carbon stocks and forest structure from Amazon forest degradation](#)

Danielle I Rappaport, Douglas C Morton, Marcos Longo et al.

- [Increased floodplain inundation in the Amazon since 1980](#)

Ayan S Fleischmann, Fabrice Papa, Stephen K Hamilton et al.

- [Robust Amazon precipitation projections in climate models that capture realistic land-atmosphere interactions](#)

J C A Baker, L Garcia-Carreras, W Buermann et al.

ENVIRONMENTAL RESEARCH
LETTERS

LETTER

Windthrow characteristics and their regional association with rainfall, soil, and surface elevation in the Amazon

OPEN ACCESS

RECEIVED
23 May 2022REVISED
20 December 2022ACCEPTED FOR PUBLICATION
29 December 2022PUBLISHED
11 January 2023

Original content from
this work may be used
under the terms of the
[Creative Commons
Attribution 4.0 licence](#).

Any further distribution
of this work must
maintain attribution to
the author(s) and the title
of the work, journal
citation and DOI.

Robinson Negron-Juarez^{1,*} , Daniel Magnabosco-Marra² , Yanlei Feng³, Jose David Urquiza-Muñoz² , William J Riley¹ and Jeffrey Q Chambers^{1,4}¹ Lawrence Berkeley National Laboratory, Climate and Ecosystem Science Division, 1 Cyclotron Road, Berkeley, CA 94720, United States of America² Max Planck Institute for Biogeochemistry, Hans Knöll Str. 10, 07745 Jena, Germany³ Carnegie Institution for Science, 260 Panama Street, Stanford, CA 94305, United States of America⁴ Department of Geography, University of California, Berkeley, CA, United States of America

* Author to whom any correspondence should be addressed.

E-mail: robinson.inj@lbl.gov**Keywords:** windthrows, geospatial analysis, AmazonSupplementary material for this article is available [online](#)**Abstract**

Windthrows (trees uprooted and broken by winds) are common across the Amazon. They range in size from single trees to large gaps that lead to changes in forest dynamics, composition, structure, and carbon balance. Yet, the current understanding of the spatial variability of windthrows is limited. By integrating remote sensing data and geospatial analysis, we present the first study to examine the occurrence, area, and direction of windthrows and the control that environmental variables exert on them across the whole Amazon. Windthrows are more frequent and larger in the northwestern Amazon (Peru and Colombia), with the central Amazon (Brazil) being another hot spot of windthrows. The predominant direction of windthrows is westward. Rainfall, surface elevation, and soil characteristics explain the variability (20%–50%) of windthrows but their effects vary regionally. A better understanding of the spatial dynamics of windthrows will improve understanding of the functioning of Amazon forests.

1. Introduction

Amazon forests absorb and store large amounts of atmospheric CO₂, thereby mitigating the warming effects of this greenhouse gas [1–3]. Tree mortality in the Amazon has increased [4, 5], and is expected to increase in a warming environment [6]. Drivers of tree mortality include, among others, deforestation [7–9], fires [10, 11], droughts [12–14] and severe storms [15–19], and these drivers are expected to become more frequent and intense [12, 20, 21]. Increases in tree mortality raise concerns due to the associated changes in carbon storage, forest structure, floristic composition and functioning of forest ecosystems [14, 22–24] and their legacies including loss of ecosystem resilience [18, 25]. This mortality has already shifted some areas to be sources of CO₂ in the Amazon [7, 26]. Drivers of natural tree mortality in the Amazon are poorly studied and represent a

key missing component of the overall tree mortality trend found in the Amazon [5].

Extreme rainfall events are a distinctive characteristic of the Amazon. These events are produced by mesoscale convective systems (MCSs) [27, 28]. Associated with MCSs are downdrafts [17, 18, 29], which are strong winds that descend from these systems [30] that can produce windthrows (trees uprooted and broken by winds [31]) when they reach the forest [30]. Windthrows in the Amazon are a recurrent form of tree mortality, ranging in size from single trees [14, 32, 33] to large gaps of uprooted and broken trees that can reach thousands of hectares [16, 18, 34–36]. Lightning is another driver of tree mortality associated with extreme rainfall that produces gaps from 3 to 11 down trees [37, 38]. Previous studies have shown that soil type, soil organic carbon (SOC) and soil nutrients have a positive association with forest gaps [37, 39, 40]. On the other hand, the effect of

topography on gaps of dead trees has contradictory effects, related not only to the type of disturbance but to the spatial scale of the analysis [40–42]. These studies suggest that controls of windthrows across the Amazon remain poorly quantified.

Changes in extreme rainfall events have the potential to alter the frequency and intensity of windthrows and related tree mortality. Despite the importance of windthrows in forest dynamics and carbon storage of the Amazon, few studies have focused on windthrow characteristics across the whole Amazon. By using Landsat images and geospatial analysis, here we present the first study of windthrow characteristics across the whole Amazon and identify (a) spatial patterns of the occurrence and size of windthrows, (b) direction of windthrows, (c) regional differences of windthrows, and (d) effects of environmental variables on the occurrence of windthrows.

2. Method and data

2.1. Study area and windthrows detection, size and direction

The study area is the Amazon rainforest ($5.65 \times 10^6 \text{ km}^2$) [18]. We used 392 Landsat 8 images (each image covering $\sim 3.4 \times 10^4 \text{ km}^2$, and $30 \text{ m} \times 30 \text{ m}$ of spatial resolution) with low cloud cover ($< 20\%$) from 2018 and 2019 (see supplementary figure S1). Windthrows were identified by their spectral characteristics [17] and distinctive fan-shape diverging from a central area [35]. To identify windthrows, spectral mixture analysis (SMA) [43] was applied to bands 2–7 in Landsat 8 images. SMA quantifies the per pixel fraction of endmembers which sums to match the full pixel spectrum of the image [43]. Image-derived endmembers of photosynthetic vegetation (PV), non-photosynthetic vegetation (NPV), and shade were used. One set of endmembers was used to identify windthrows across the whole Amazon (figure S2). The fractions of PV and NPV were then normalized without shade as $PV/(PV + NPV)$ and $NPV/(PV + NPV)$ [44]. The normalized NPV and PV images were used to identify new and old windthrows, respectively. Each identified windthrow was verified using historical Landsat images dating back to 1984. Windthrows were visually verified for their fan-shape (diverging from a central area with small pixels scattered at the tail). For this task we used a band combination RGB as shortwave infrared ($1.57\text{--}1.65 \mu\text{m}$), near infrared ($0.85\text{--}0.88 \mu\text{m}$) and red ($0.64\text{--}0.67 \mu\text{m}$). In this band composition, old windthrows look bright green (due to the presence of pioneers that reflect more near infrared [45]) and new windthrows (< 1 year old) look red (due to high shortwave infrared reflectance from exposed bare wood) (figure S3). The 2018–2019 Landsat images used encompass new windthrows as well as old windthrows in the Amazon for a period

of ~ 30 years since the Landsat reflectance recover to pre-disturbance conditions in about 40 years in the central Amazon [45, 46] and about 20 years in the western Amazon [47]. We only considered windthrows that were further than 5 km from human settled areas. In total we identified 1116 windthrows.

To determine windthrow area, the main gap of each windthrow was manually delineated by a triangle with one vertex in the beginning of the fan-shaped windthrow and the other vertices at the extreme ends of the fan (figure S3). The area of the windthrow was determined by the area of its respective triangle. The selection of Landsat 8 images (Landsat 8 Collection 2 Tier 1 calibrated top-of-atmosphere, TOA, reflectance) with less than 20% of cloud cover, the SMA analysis, the delineation of the windthrows area, and the calculation of their area with their respective centroid were done in the Google Earth Engine (GEE) platform [48] that provides tools and algorithms for these tasks. Only windthrows larger than 5 ha were used in our analysis. The direction of the windthrow was determined from the vertex (tail) representing the beginning of the fan-shaped windthrow to the middle of the side connecting the other vertices (figure S3). We used the geographic convention of true north as 0° with the angle increasing clockwise.

2.2. Environmental data

2.2.1. Rainfall data

We used the Tropical Rainfall Measuring Mission (TRMM) Multi-Satellite Precipitation (TMPA) rainfall Level 3 V7 $0.25^\circ \times 0.25^\circ$ 3 h (3B42) and monthly (3B43) data [49] from 1 January 1998 to 31 December 2018, available at <https://disc.gsfc.nasa.gov/datasets/>. TRMM data compare well with observations in tropical forests [50, 51]. The TRMM satellite stopped collecting data in 2015. TRMM-like data were processed using the successor satellite, the Global Precipitation Measurement [49, 52] until 2019. The mean annual number of extreme rainfall rate events (MAN-ERR) per pixel was calculated using TRMM 3B42 by adding the number of rainfall rate events $\geq 6 \text{ mm h}^{-1}$ (extreme rainfall produced by MCSs [28]) per pixel and dividing this total by the number of years used. TRMM 3B43 was used to calculate the mean annual rainfall (MAR) as the average of total annuals. Dry season length was calculated from TRMM 3B43 data by computing the mean monthly rainfall and from there the number of months with rainfall $\leq 100 \text{ mm}$ per month [53].

2.2.2. Soil classification

Variations of physical and chemical properties of soil strongly affect trees and root growth [54, 55], and therefore might affect the response of trees to winds. The Harmonized World Soil Database (HWSD) v1.21 [56] was used to determine the soil classification. The HWSD is a 30 arc second ($\sim 1 \text{ km}$) resolution dataset

that combines current regional and national-level soil data from around the world. The data are available at www.fao.org/soils-portal/data-hub/soil-maps-and-databases/harmonized-world-soil-database-v12/en/.

2.2.3. Soil properties

The SOC pool is driven by the rates of organic inputs [54, 57] of decomposition that in turn facilitate nutrient availability such as nitrogen and phosphorous. Disturbances can result in a dramatic increase in organic matter inputs into soils [58, 59] with associated effects on soil nutrients. Previous studies have shown that soil carbon and nutrients decay exponentially with depth in the Amazon, with the upper 15 cm having the highest values [54]. Therefore, we used SOC and soil organic nitrogen (SON) from these layers. SOC and SON were obtained from SoilGrids 2.0 which is a global digital soil mapping database with a spatial resolution of 250 m and multiple depths [60]. These data are available in GEE (https://git.wur.nl/isric/soilgrids/soilgrids.notebooks/-/blob/master/markdown/access_on_gee.md).

2.2.4. Elevation

Tree mortality varies inversely with surface elevation [61, 62]. Soil elevation data is from Advanced Land Observing Satellite (ALOS) World 3D (AW3D30) Version 3.2 which is a global digital surface model (DSM) with a horizontal resolution of 30 m (1 arcsec) [63]. The Japan Aerospace Exploration Agency (JAXA) generated these global digital elevation/surface model (DEM/DSM) and orthorectified images using the archived data of the Panchromatic Remote-sensing Instrument for Stereo Mapping onboard ALOS. These data are available in GEE (ee.ImageCollection("JAXA/ALOS/AW3D30/V3_2")).

2.2.5. Landform classification

Landform classification data is from height above the nearest drainage (HAND) and provides the vertical distance from hillslope to nearest stream [64, 65]. HAND could be an indicator of whether windthrows are more or less likely in areas of low or high elevation. The HAND data used a one arc-second (~ 30 m) resolution version of Shuttle Radar Topography Mission [66]. The data are available in GEE ([users/gena/global-hand/hand-100](https://users.gena/global-hand/hand-100)).

2.2.6 Temperature

Trees respond to their climate. The association between tree gaps and temperature is investigated through the mean annual temperature (MAT) (1998–2018). MAT data is from the Climatic Research Unit Version 4, CRU v4 which has a spatial resolution of 0.5° and is derived from the interpolation of monthly data from an extensive network

of weather stations [67]. The data are available at <https://crudata.uea.acuk/cru/data/temperature/>.

2.2.7. Canopy height

The proportion of trees exposed to wind is related to their height. We used data derived from global spaceborne lidar available at a spatial resolution of 1 km using 2005 data from the Geoscience Laser Altimeter System aboard Ice, Cloud, and land Elevation Satellite [68]. The data is available in GEE (ee.Image("NASA/JPL/global_forest_canopy_height_2005")).

2.2.8. Wind speed

Horizontal wind speed data are from ERA5 (European Centre for Medium-Range Weather Forecasts Reanalysis v5) which has a detailed record of atmospheric, land surface and ocean measurements from 1950 onward at a horizontal resolution of 0.1° [69]. We used the average land monthly data of the 10 m u - and v -wind components (in ms^{-1}) for the period 1998–2018. u is the component of wind parallel to the x -axis and v is the component of wind parallel to the y -axis. The u and v wind components were averaged separately to obtain the mean annual component where the annual average wind speed was calculated ($\text{wind speed} = \sqrt{u_{\text{average}}^2 + v_{\text{average}}^2}$). Data is available at www.ecmwf.int/en/forecasts/datasets/reanalysis-datasets/era5.

Table S1 summarize the data used. Figure S4 shows the suite of environmental data in our study area.

2.3. Procedures

2.3.1. Density of windthrow occurrence and size

Our study focuses on the regional variation of windthrows over the entire Amazon, therefore we used a spatial resolution of 0.1° to capture the variation across different regions in the Amazon, a desirable characteristic when choosing spatial resolution [70]. Using 0.1° resolution, we found that 934 individual windthrows were inside one grid cell, in 81 cases two windthrows coincided in one cell, and in 7 cases three windthrows. When windthrows coincided in the same grid cell then only one windthrows was randomly selected. After this procedure we had one windthrows per cell, totaling 1022. The density of the occurrence of windthrows and their sizes were calculated by applying a kernel density estimator [71] using the System for Automated Geoscientific Analyses geospatial library available in Quantum Geographic Information System (QGIS, version 3.10 that is freely available at <https://qgis.org>) using a quartic kernel with 1° radius and resampled to 0.1° .

2.4. Windthrows and environmental data

The environmental data were resampled to 0.1° , to match the windthrow density resolution. The resampling used the cubic spline resampling method on all datasets except for the Soil Classification data which was resampled using the nearest neighbor method, a common practice for categorical data [70]. The resampling was done in QGIS. The spline resampling method produces reliable resampling results for climate [72] and topographic [73] data. The environmental data used here are the best data currently available for the Amazon and properly represent the climatic, edaphic, topographic, and forest structural characteristics observed in the Amazon [74]. The availability and continuous improvement of these data are key to understanding the dynamics of this ecosystem.

2.4.1. Spatial autocorrelation, regionalization, and spatial regression

Each windthrow was used to locate the associated density and respective environmental variables. We used Moran's I [75] to measure the global spatial autocorrelation of the data. Windthrows are multivariate processes because they are affected by numerous factors. In order to analytically identify spatial patterns of windthrows and their environmental variables, we used regionalization. Regionalization uses unsupervised learning methods to identify spatial structures of multivariate processes and aggregates areas into contiguous regions that have internal homogenous characteristics with all regions being statistically different among them [76–78]. Prior to regionalization, the data were standardized using a robust scaling method, where each variable has the median subtracted and divided by the interquartile range (the difference between the 75th and 25th percentiles) [79]. The spatial criterion is structured by spatial weight. We used two spatial weights matrices, the queen contiguity matrix (Queen) where observations are connected to neighbors they touch, and the k-nearest neighbor matrix (KNN) where observations are connected to their fourth nearest observations. For the regionalization we used the Ward's hierarchical method, an agglomerative hierarchical clustering method that minimizes the total within-cluster variance [80]. We used the Calinski-Harabasz score (CH) [81] to assess the goodness of fit for the regions obtained. Higher CH values indicate better fits [81].

A spatial regression was performed using the density of windthrows occurrence (hereafter referred to as windthrow density) as the independent variable (predictant). We used a spatial regression model based on ordinary least squares to compute the regression coefficients. To assess the spatial dependence, we used the Lagrange multiplier (LM) (lag and

error) statistics. If Lagrange statistics were not significant then we used Robust LM (lag and error) statistics. If Robust lag was significant and Robust error was not, then a spatial error model was used, in the opposite case a spatial lag model was used. In the case that statistics were significant then the statistic with highest value was used. Details of the statistical flow used in this study are found in Anselin and Rey [82]. The regionalization and spatial regression were done using the Python Library of Spatial Analytical Methods, PySAL [83].

3. Results

3.1. Windthrows characteristics

The highest windthrow density (figure 1(A)) was observed in the northwestern (Peru and Colombia) and central (Brazil) Amazon, and regions with lower occurrence were observed in the northern (Venezuela, Guyana, Suriname and French Guiana), eastern (Brazil) and southern (Peru, Bolivia and Brazil) Amazon. The largest windthrows were observed in the northwestern Amazon followed by the central Amazon (figure 1(B)). We found that most windthrows (81% of cases) have a westward component (figure 1(C)). A map with the direction of each windthrow is shown in figure S5.

3.2. Regions of windthrows

Using regionalization analysis, we found the highest CH score (table S2) was using windthrow density, Elevation, SOC stock from 0–5 cm depth, and MAR (figure 2). The Moran's I value was >0.7 ($p = 0.001$) for these variables suggesting clear spatial structures with non-random distributions.

The Queen weighting method yielded the best regionalization results (table S2). The four Regions obtained using this method are shown in figure 3 (results using the KNN method are in figure S6). The distribution profile of each variable for each Region is shown in figure S7. The number of windthrows contained in Regions 1, 2, 3, and 4 were 390, 291, 297, and 44, respectively. Using 5 regions we obtained CH scores of 256 and 277 using the Queen weighting and KNN methods, respectively.

3.3. Explanatory variables

Using the results from our regionalization analysis, we determined an association between windthrow density, the predictant, and predictors (Elevation, SOC stock from 0–5 cm, and MAR). No multicollinearity was observed in the models (table S3). The F-statistic showed that all models were significant and have predictive capabilities (probability < 0.05), except for Region 4 (probability = 0.5) (figure 4). The errors from the models with respect to observations were normally distributed around zero

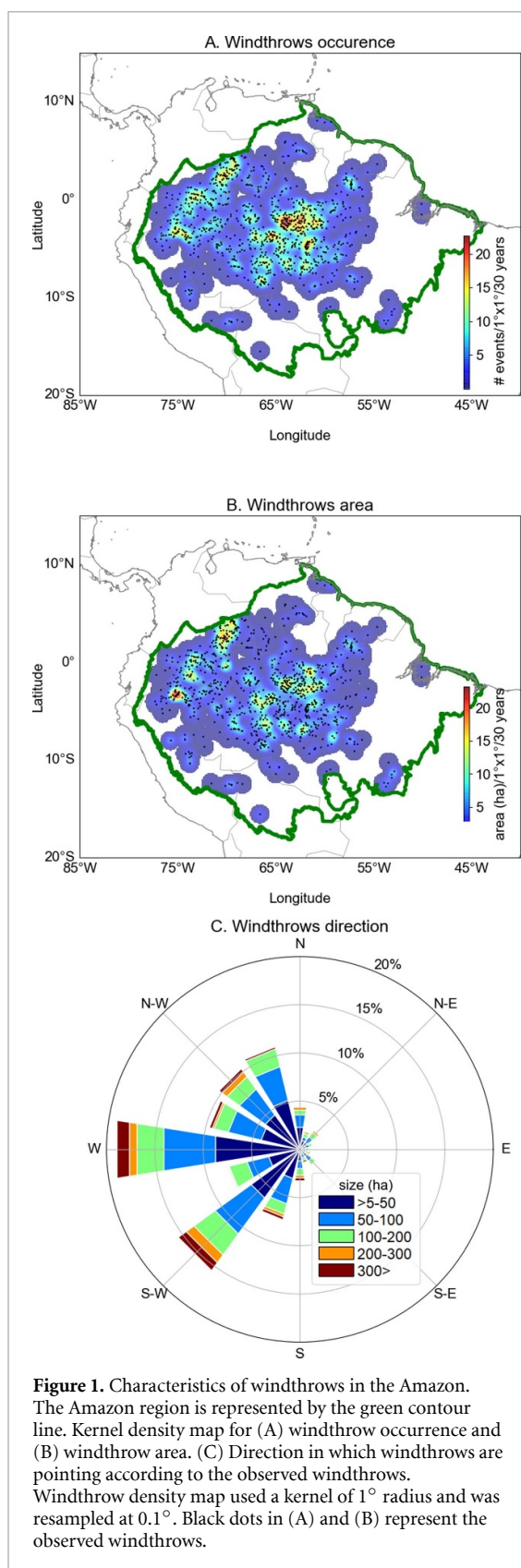


(figure S8), indicating no critical under- and over-estimates. The results showed that windthrows are positively correlated with MAR (except in Region 2), but vary inversely with Elevation (except in Region 4) and SOC. Overall, MAR and Elevation contribute the most (largest magnitude) in the prediction of

windthrows. Across the whole Amazon the predictors explained 11% of windthrows density (figure 4(E)).

4. Discussions and conclusions

4.1. Windthrows characteristics

Windthrows were common from the rainy northwest to the dry southeast Amazon. The high occurrence of windthrows in the central Amazon is consistent with a recent study of small forest gaps in this region [40] and was not identified in previous studies [35, 36] that used a threshold windthrow size of 30 ha which might have underestimated the occurrence of windthrows. Only one study has focused on the spatial-temporal variability of windthrows in the central Amazon for the period 1998–2010 [84]. That study did not find an increase of windthrows, suggesting that if an increase has occurred it has happened after 2010. Nevertheless, an increase in windthrows would be consistent with the observed increase in tree mortality found in inventory plots across the Amazon [5] and could provide insights into the mechanisms underlying this trend. An increase in the frequency of windthrows in the central Amazon could promote changes in the regional floristic composition as shown in Negron-Juarez *et al* [18]. Our study included only windthrows >5 ha but windthrows cover a large spectrum of disturbances including single downed trees. Integration of field and remote sensing data (e.g. LiDAR, Landsat, etc), is needed in order to determine the fraction of tree mortality associated with winds in the Amazon. Such integration will provide a better understanding of the Amazon. For instance, by including wind induced tree mortality, we found that the forest dynamics associated with these events properly represent the values of biomass in the central Amazon [16]. Our results also showed a low number of MANERR in the northeastern Amazon (1.5° N, 53° W) (figure S4), an area where recent studies have found trees taller than 80 m [85].

Our study showed that windthrows in the Amazon have a preferential east to west direction (figure 1(C)). This direction coincides with the dominant direction of MCSs in the Amazon [27]. On the other hand, windthrows with an easterly direction are less frequent and can be related to the lower frequency of easterly MCSs [84]. These results suggest that MCSs are key drivers of windthrows and complement previous studies that found squall lines (i.e. aligned bands of MCSs) [86] to be the drivers of windthrows [17, 29, 84], despite the fact that squall lines are not common in the northwestern Amazon [86], a region where we found a large amount of windthrows.

4.2. Regionalization

Regions 1 and 3 were characterized by elevations < 300 meters above sea level and a lower number of extreme rainfall events than the western

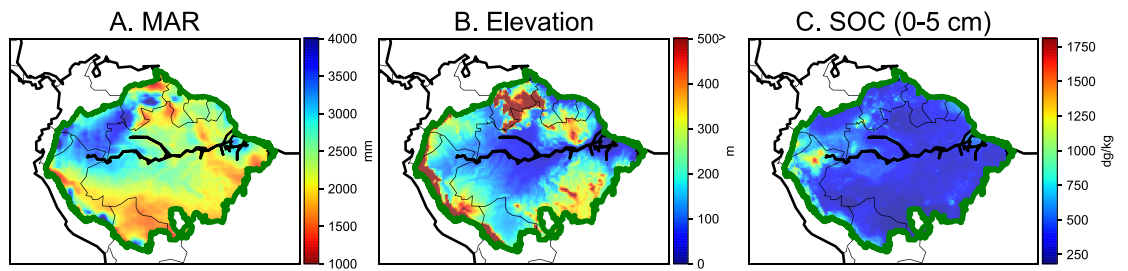


Figure 2. Environmental variables used to explain windthrow density in the Amazon. (A) Mean annual rainfall (MAR), (B) surface elevation, and (C) soil organic carbon (SOC) in the 0–5 cm soil layer.

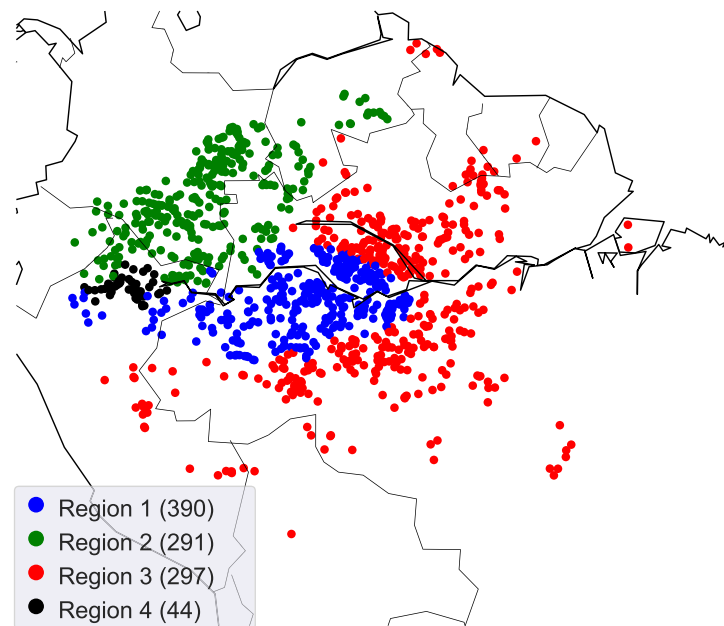


Figure 3. Windthrow regions in the Amazon determined by a regionalization analysis. The regionalization analysis used the queen weighting method. The number of windthrows in regions 1–4 are 390, 291, 297, and 44, respectively.

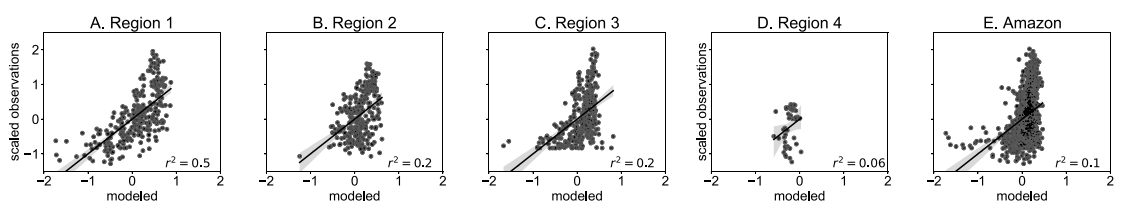


Figure 4. Comparison of observed versus modeled windthrow density for the four Regions determined through regionalization (figure 3), and the whole Amazon. All regressions were statistically significant ($p < 0.05$), except for Region 4 and the whole Amazon. Statistical details for all regions are shown in table S3.

Amazon (figure 2(B)). These Regions appear to have the most severe storms across the Amazon as suggested by the high values of convective available potential energy [87], and more frequent lightning [88]. Observational studies have shown that during the wet season, rainfall occurs independent of elevation; however, differences on the order of 100 m in surface elevation could provide the forcing for cloud formation during the dry season [89]. Regions 2 and 4 are located in the northwest part of the Amazon, an area characterized by higher elevations, due to

its proximity to the Andes. These two Regions had the largest values of MAR (and MANERR) because higher elevation favors higher rainfall. This is due to the subsidence of thermal heating which allows an increase in convection that organizes into MCSs [90]. However, the closer a region is to the Andes, the lower the rainfall, as rainfall decreases with elevation [91]. The patterns we report here require further investigation spanning temporal scales since trends in extreme rainfall have been observed across the Amazon due to deforestation and climate variability [92].

Table 1. Coefficients of environmental variables obtained from OLS regression. Full statistics results are shown in table S3. Non-significant F-statistics given in italics.

	MAR	Elevation	SOC 0–5 cm	r^2	F-statistic
Region 1	0.1	−0.6	−0.1	0.5	87.7
Region 2	−0.13	−0.04	−0.04	0.2	19.7
Region 3	0.17	−0.23	−0.02	0.2	37.5
Region 4	0.17	0.07	−0.1	0.06	<i>0.88</i>
Amazon	0.06	−0.18	−0.11	0.1	50.6

4.3. Regressions

Windthrow correlated positively with MAR. In general, rainfall can promote saturated soils that in turn limit the anchoring of trees making them more sensitive to winds [18]. Regions 2 and 4 have a high frequency of extreme rainfall events (figure S4), and a high occurrence of windthrows. Coincidentally, in these Regions studies have shown a low tree residence time (high tree mortality) [22]. On the other hand Regions 1 and 3 appear to have the most severe storms [88] which might help to explain the high occurrence of windthrows in these Regions. In Region 2, maximum MAR values were observed in an area with low elevation in the border between Colombia, Brazil and Venezuela where the relief shape and concavity of the Andes promote air convergence and high rainfall [93, 94]. Associated with this high rainfall is cloud cover (figure S1) that might have influenced the low number of identified windthrows along the border between these countries.

Windthrows vary inversely with elevation. A decrease in tree mortality with elevation was found in the tropical forest of Borneo [95]. A decrease in tree mortality with elevation was also found in inventory plots in other tropical forests [42, 96]. Furthermore, observational studies have shown that wood density increases with elevation [95, 97–99], and therefore these trees are less vulnerable to winds [99, 100]. Similarly, trees in plateaus have deeper root systems [101, 102] resulting in stronger tree anchoring. These studies suggest that, apart from tree-soil interactions and differential exposure to wind gusts, variations in tree mortality across topography are likely to reflect the vertical heterogeneity of the forest canopy, as well as interactions among trees, lianas, and epiphytes, which can influence the mechanical stability and anchoring efficiency. In Region 4 windthrows vary positively with elevation but this effect is very small and was not significant. Our results corroborate the important and complex role of elevation on the occurrence of windthrows.

Windthrows vary inversely with SOC. The occurrence of windthrows implies the presence of dead trees and therefore SOC [59, 103] and nutrient availability [104] dependencies. Studies have shown that large amounts of rainfall promote accumulation of SOC [105, 106], explaining the large amounts of

SOC in the northwestern Amazon (figure 2(C)). A decrease in SOC is observed from Regions 2 and 4, in contrast to the increases in windthrows in those regions (figure 1(B)). Similarly, an increase in SOC is observed from east to west in Regions 1 and 3 (figure 2(C)), in contrast to a high density of windthrows in the eastern-central part of the Amazon (figure 1(A)). These patterns explain the negative association between windthrows and SOC (table 1). Previous studies suggest that SOC, nitrogen (N) and phosphorous (P), are related [39, 107], suggesting that the effect of N and P on windthrows might be similar to that of SOC.

Windthrows have the potential to change forest composition in the Amazon [18]. Forest composition influences the climate feedback from cloud formation and rain to carbon uptake [108–111]. Since rainfall has a direct effect on the occurrence of windthrows, we suggest that Earth system models should include the effects of windthrows to reduce uncertainties on the projected functionality of the Amazon in the future.

4.4. Final remarks

Intrinsic to windthrows is the fact that forested surfaces facing the direction of the storms have the most windthrown trees as shown in our previous studies [17, 18, 112, 113]. Westward MCSs will have a larger impact on surfaces with an eastern aspect, and eastward MCSs will affect largely western-facing surfaces. Thus, it has been suggested that aspect (the direction that a terrain surface faces) is not an explanatory variable, but rather a factor [114]. Aspect in the Amazon is a local characteristic that can produce misleading results after upscaling since several aspect values will be averaged together, muting their effect [115]. We estimate that about 10%–15% of all windthrows identified did not have a clear fan shape, and were not included in the total number of windthrows identified (1116). A more comprehensive regression or machine learning analysis should explore the effect of endogenous variables as well as different regimes in each of the selected regions. Regimes analysis implies that in each Region the regression model changes due to the spatial heterogeneity of the data [82]. We found that windthrows in the Amazon have regional characteristics of occurrence and size, and further

analyses are needed to understand the causes of these characteristics.

Data availability statement

All data that support the findings of this study are included within the article (and any supplementary files).

Acknowledgments

This study was supported by the Office of Science, Office of Biological and Environmental Research of the US Department of Energy, Agreement Grant. DE-AC02-05CH11231, Next Generation Ecosystem Experiments-Tropics, and the Office of Science's Regional and Global Model Analysis of the US Department of Energy, Agreement Grant. DE-AC02-05CH11231, Reducing Uncertainties in Biogeochemical Interactions through Synthesis Computation Scientific Focus Area (RUBISCO SFA). DMM was supported by German Federal Ministry of Education and Research, Grants 01LB1001A and 01LK1602A. JDUM was supported by the Max Planck Institute of Biogeochemistry and the DAAD (German Academic Exchange Service). Landsat Imagery was analyzed using the Google Earth Engine: A planetary-scale geospatial analysis platform, Google Earth Engine Team 2015, <https://earthengine.google.com>. RNJ thanks Megan McGroddy for discussions of soil nutrients related to this study.


Conflict of interest


All the authors declare they have no competing interests.

ORCID iDs

Robinson Negron-Juarez  <https://orcid.org/0000-0002-4691-2692>

Daniel Magnabosco-Marra  <https://orcid.org/0000-0003-1216-2982>

Jose David Urquiza-Muñoz  <https://orcid.org/0000-0002-0062-2278>

William J Riley  <https://orcid.org/0000-0002-4615-2304>

References

- Pan Y, Birdsey R A, Phillips O L and Jackson R B 2013 The structure, distribution, and biomass of the world's forests *Annu. Rev. Ecol. Evol. Syst.* **44** 593–622
- Fernandez-Martinez M, Vicca S, Janssens I A, Luysaert S, Campioli M, Sardans J, Estiarte M and Peñuelas J 2014 Spatial variability and controls over biomass stocks, carbon fluxes, and resource-use efficiencies across forest ecosystems *Trees* **28** 597–611
- Malhi Y, Doughty C and Galbraith D 2011 The allocation of ecosystem net primary productivity in tropical forests *Phil. Trans. R. Soc. B* **366** 3225–45
- Bullock E L, Woodcock C E, Souza C and Olofsson P 2020 Satellite-based estimates reveal widespread forest degradation in the Amazon *Glob. Change Biol.* **26** 2956–69
- Brienen R J W et al 2015 Long-term decline of the Amazon carbon sink *Nature* **519** 344
- McDowell N et al 2018 Drivers and mechanisms of tree mortality in moist tropical forests *New Phytol.* **219** 851–69
- Gatti L V et al 2021 Amazonia as a carbon source linked to deforestation and climate change *Nature* **595** 388
- Malhi Y, Roberts J T, Betts R A, Killeen T J, Li W H and Nobre C A 2008 Climate change, deforestation, and the fate of the Amazon *Science* **319** 169–72
- Silva C H L, Pessoa A C M, Carvalho N S, Reis J B C, Anderson L O and Aragao L 2021 The Brazilian Amazon deforestation rate in 2020 is the greatest of the decade *Nat. Ecol. Evol.* **5** 144–5
- Brando P M et al 2014 Abrupt increases in Amazonian tree mortality due to drought-fire interactions *Proc. Natl Acad. Sci. USA* **111** 6347–52
- Aragao L et al 2018 21st Century drought-related fires counteract the decline of Amazon deforestation carbon emissions *Nat. Commun.* **9** 536
- Duffy P B, Brando P, Asner G P and Field C B 2015 Projections of future meteorological drought and wet periods in the Amazon *Proc. Natl Acad. Sci. USA* **112** 13172–7
- de Oliveira B F A, Bottino M J, Nobre P and Nobre C A 2021 Deforestation and climate change are projected to increase heat stress risk in the Brazilian Amazon *Commun. Earth Environ.* **2** 207
- Esquivel-Muelbert A et al 2020 Tree mode of death and mortality risk factors across Amazon forests *Nat. Commun.* **11** 5515
- Singh M S, Kuang Z M, Maloney E D, Hannah W M and Wolding B O 2017 Increasing potential for intense tropical and subtropical thunderstorms under global warming *Proc. Natl Acad. Sci. USA* **114** 11657–62
- Chambers J Q, Negron-Juarez R I, Magnabosco Marra D, Di Vittorio A, Tews J, Roberts D, Ribeiro G H P M, Trumbore S E and Higuchi N 2013 The steady-state mosaic of disturbance and succession across an old-growth central Amazon forest landscape *Proc. Natl Acad. Sci. USA* **110** 3949–54
- Negrón-Juárez R I, Chambers J Q, Guimaraes G, Zeng H, Raupp C F M, Magnabosco Marra D, Ribeiro G H P M, Saatchi S S, Nelson B W and Higuchi N 2010 Widespread Amazon forest tree mortality from a single cross-basin squall line event *Geophys. Res. Lett.* **37** L16701
- Negrón-Juárez R I et al 2018 Vulnerability of Amazon forests to storm-driven tree mortality *Environ. Res. Lett.* **13** 054021
- Espirito-Santo F D B, Keller M, Braswell B, Nelson B W, Frolking S and Vicente G 2010 Storm intensity and old-growth forest disturbances in the Amazon region *Geophys. Res. Lett.* **37** L11403
- IPCC 2022 *Climate Change 2022: Impacts, Adaptation and Vulnerability. Contribution of Working Group II to the Sixth Assessment Report of the Intergovernmental Panel on Climate Change* (Cambridge University Press) (<https://doi.org/10.1017/9781009325844>)
- Baker J C A, Garcia-Carreras L, Buermann W, de Souza D C, Marsham J H, Kubota P Y, Gloor M, Coelho C A S and Spracklen D V 2021 Robust Amazon precipitation projections in climate models that capture realistic land-atmosphere interactions *Environ. Res. Lett.* **16** 074002
- Franklin J F, Shugart H H and Harmon M E 1987 Tree death as an ecological process *Bioscience* **37** 550–6
- Galbraith D et al 2013 Residence times of woody biomass in tropical forests *Plant Ecol. Divers.* **6** 139–57
- Sturtevant B R and Fortin M-J 2021 Understanding and modeling forest disturbance interactions at the landscape level *Front. Ecol. Evol.* **9** 653647

- [25] Buma B 2015 Disturbance interactions: characterization, prediction, and the potential for cascading effects *Ecosphere* **6** 1–15
- [26] Berenguer E et al 2021 Tracking the impacts of El Niño drought and fire in human-modified Amazonian forests *Proc. Natl Acad. Sci. USA* **118**
- [27] Rehbein A, Ambrizzi T and Mechoso C R 2018 Mesoscale convective systems over the Amazon basin. Part I: climatological aspects *Int. J. Climatol.* **38** 215–29
- [28] Jaramillo L, Poveda G and Mejia J F 2017 Mesoscale convective systems and other precipitation features over the tropical Americas and surrounding seas as seen by TRMM *Int. J. Climatol.* **37** 380–97
- [29] Garstang M, White S, Shugart H H and Halverson J 1998 Convective cloud downdrafts as the cause of large blowdowns in the Amazon rainforest *Meteorol. Atmos. Phys.* **67** 199–212
- [30] Fujita T T 1990 Downbursts—meteorological features and wind-field characteristics *J. Wind Eng. Ind. Aerodyn.* **36** 75–86
- [31] Mitchell S J 2013 Wind as a natural disturbance agent in forests: a synthesis *Forestry* **86** 147–57
- [32] de Toledo J J, Magnusson W E and Castilho C V 2013 Competition, exogenous disturbances and senescence shape tree size distribution in tropical forest: evidence from tree mode of death in central Amazonia *J. Veg. Sci.* **24** 651–63
- [33] Aubry-Kientz M, Rossi V, Wagner F and Herault B 2015 Identifying climatic drivers of tropical forest dynamics *Biogeosciences* **12** 5583–96
- [34] Negrón-Juárez R I, Chambers J Q, Magnabosco Marra D, Ribeiro G H P M, Rifai S W, Higuchi N and Roberts D 2011 Detection of subpixel treefall gaps with Landsat imagery in central Amazon forests *Remote Sens. Environ.* **115** 3322–8
- [35] Nelson B W, Kapos V, Adams J B, Oliveira W and Braun O 1994 Forest disturbance by large blowdowns in the Brazilian Amazon *Ecology* **75** 853–8
- [36] Espirito-Santo F D B et al 2014 Size and frequency of natural forest disturbances and the Amazon forest carbon balance *Nat. Commun.* **5** 3434
- [37] Yanoviak S P, Gora E M, Bitzer P M, Burchfield J C, Muller-Landau H C, Detto M, Paton S and Hubbell S P 2020 Lightning is a major cause of large tree mortality in a lowland neotropical forest *New Phytol.* **225** 1936–44
- [38] Fontes C G, Chambers J Q and Higuchi N 2018 Revealing the causes and temporal distribution of tree mortality in central Amazonia *For. Ecol. Manage.* **424** 177–83
- [39] Soong J L et al 2020 Soil properties explain tree growth and mortality, but not biomass, across phosphorus-depleted tropical forests *Sci. Rep.* **10**
- [40] Dalagnol R, Wagner F H, Galvao L S, Streher A S, Phillips O L, Gloor E, Pugh T A M, Ometto J P H B and Aragão L E O C 2021 Large-scale variations in the dynamics of Amazon forest canopy gaps from airborne lidar data and opportunities for tree mortality estimates *Sci. Rep.* **11** 1388
- [41] Cushman K C, Detto M, Garcia M, Muller-Landau H C and Coulson T 2022 Soils and topography control natural disturbance rates and thereby forest structure in a lowland tropical landscape *Ecol. Lett.* **25** 1126–38
- [42] de Toledo J J, Magnusson W E, Castilho C V and Nascimento H E M 2012 Tree mode of death in central Amazonia: effects of soil and topography on tree mortality associated with storm disturbances *For. Ecol. Manage.* **263** 253–61
- [43] Adams J B et al 1995 Classification of multispectral images based on fractions of endmembers—application to land-cover change in the Brazilian Amazon *Remote Sens. Environ.* **52** 137–54
- [44] Adams J B and Gillespie A R 2006 *Remote Sensing of Landscapes with Spectral Images: A Physical Modeling Approach* (Cambridge: Cambridge University Press) (<https://doi.org/10.1017/CBO9780511617195>)
- [45] Negron-Juarez R, Holm J A, Faybishenko B, Magnabosco-Marra D, Fisher R A, Shuman J K, de Araujo A C, Riley W J and Chambers J Q 2020 Landsat near-infrared (NIR) band and ELM-FATES sensitivity to forest disturbances and regrowth in the central Amazon *Biogeosciences* **17** 6185–205
- [46] Magnabosco Marra D et al 2018 Windthrows control biomass patterns and functional composition of Amazon forests *Glob. Change Biol.* **24** 5867–81
- [47] Urquiza Muñoz J D et al 2021 Recovery of forest structure following large-scale windthrows in the northwestern Amazon *Forest* **12** 667
- [48] Gorelick N, Hancher M, Dixon M, Ilyushchenko S, Thau D and Moore R 2017 Google Earth Engine: planetary-scale geospatial analysis for everyone *Remote Sens. Environ.* **202** 18–27
- [49] Huffman G J et al 2018 NASA global precipitation measurement (GPM) integrated multi-satellite retrievals for GPM (IMERG) *Algorithm Theoretical Basis Document (ATBD) Version 5.2* (Greenbelt, MD: NASA)
- [50] Munzimi Y A, Hansen M C, Adusei B and Senay G B 2015 Characterizing Congo basin rainfall and climate using Tropical Rainfall Measuring Mission (TRMM) satellite data and limited rain gauge ground observations *J. Appl. Meteorol. Climatol.* **54** 541–55
- [51] Negrón-Juárez R I, Li W, Fu R, Fernandes K and Cardoso Ad O 2009 Comparison of precipitation datasets over the tropical south American and African continents *J. Hydrometeorol.* **10** 289–99
- [52] Skofronick-Jackson G et al 2017 The global precipitation measurement (GPM) mission for science and society *Bull. Am. Meteorol. Soc.* **98** 1679–95
- [53] Sombroek W 2001 Spatial and temporal patterns of Amazon rainfall—consequences for the planning of agricultural occupation and the protection of primary forests *Ambio* **30** 388–96
- [54] Quesada C A, Lloyd J, Anderson L O, Fyllas N M, Schwarz M and Czimczik C I 2011 Soils of Amazonia with particular reference to the RAINFOR sites *Biogeosciences* **8** 1415–40
- [55] Quesada C A et al 2012 Basin-wide variations in Amazon forest structure and function are mediated by both soils and climate *Biogeosciences* **9** 2203–46
- [56] FAO 2012 Harmonized world soil database (version 1.2) (Rome and IIASA, Laxenburg: Food Agriculture Organization) (available at: <http://webarchive.iiasa.ac.at/Research/LUC/External-World-soil-database/HTML/>)
- [57] Trumbore S E, Davidson E A, Decamargo P B, Nepstad D C and Martinelli L A 1995 Belowground cycling of carbon in forest and pastures of eastern Amazonia *Glob. Biogeochem. Cycles* **9** 515–28
- [58] Grau O et al 2017 Nutrient-cycling mechanisms other than the direct absorption from soil may control forest structure and dynamics in poor Amazonian soils *Sci. Rep.* **7**
- [59] Vitousek P M and Denslow J S 1986 Nitrogen and phosphorus availability in treefall gaps of a lowland tropical rain-forest *J. Ecol.* **74** 1167–78
- [60] Poggio L, de Sousa L M, Batjes N H, Heuvelink G B M, Kempen B, Ribeiro E and Rossiter D 2021 SoilGrids 2.0: producing soil information for the globe with quantified spatial uncertainty *Soil* **7** 217–40
- [61] Stephenson N L, van Mantgem P J, Bunn A G, Bruner H, Harmon M E, O'Connell K B, Urban D L and Franklin J F 2011 Causes and implications of the correlation between forest productivity and tree mortality rates *Ecol. Monogr.* **81** 527–55
- [62] de Toledo J J, Magnusson W E, Castilho C V and Nascimento H E M 2011 How much variation in tree mortality is predicted by soil and topography in central Amazonia? *For. Ecol. Manage.* **262** 331–8
- [63] Takaku J, Tadoro T, Doutsu M and Kai H 2020 Updates of 'AW3D30' ALOS global digital surface model with other

- open access datasets *Int. Arch. Photogramm. Remote Sens. Spat. Inf. Sci. ISPRS* **43** 183–9
- [64] Renno C D, Nobre A D, Cuartas L A, Soares J V, Hodnett M G, Tomasella J and Waterloo M J 2008 HAND, a new terrain descriptor using SRTM-DEM: mapping terra-firme rainforest environments in Amazonia *Remote Sens. Environ.* **112** 3469–81
- [65] Nobre A D, Cuartas L A, Hodnett M, Renno C D, Rodrigues G, Silveira A, Waterloo M and Saleska S 2011 Height above the nearest drainage—a hydrologically relevant new terrain model *J. Hydrol.* **404** 13–29
- [66] Donchyts G et al 2016 Global 30m height above the nearest drainage *European Geosciences Union* (Vienna: EGU)
- [67] Harris I, Osborn T J, Jones P and Lister D 2020 Version 4 of the CRU TS monthly high-resolution gridded multivariate climate dataset *Sci. Data* **7** 56
- [68] Simard M, Pinto N, Fisher J B and Baccini A 2011 Mapping forest canopy height globally with spaceborne lidar *J. Geophys. Res.* **116** G04021
- [69] Hersbach H et al 2020 The ERA5 global reanalysis *Q. J. R. Meteorol. Soc.* **146** 1999–2049
- [70] Atkinson P M 2017 Spatial Resolution *The International Encyclopedia of Geography* ed D Richardson, N Castree, M Goodchild, A Kobayashi, W Liu and R Marston (New York: Wiley) p 217
- [71] Rosenblatt M 1956 Remarks on some nonparametric estimates of density-function *Ann. Math. Stat.* **27** 832–7
- [72] Sharifi E, Saghafian B and Steinacker R 2019 Downscaling satellite precipitation estimates with multiple linear regression, artificial neural networks, and spline interpolation techniques *J. Geophys. Res.* **124** 789–805
- [73] Boreggio M, Bernard M and Gregoretti C 2018 Evaluating the differences of gridding techniques for Digital Elevation Models generation and their influence on the modeling of stony debris flows routing: a case study from Rovina di Cancia basin (North-eastern Italian Alps) *Front. Earth Sci.* **6** 89
- [74] Malhi Y and Davidson E A 2009 Biogeochemistry and ecology of terrestrial ecosystem of Amazonia *Amazonia and Global Change Geophysical Monograph* ed M Keller, M Bustamante, J Gash and P Silva Dias (Washington, DC: American Geophysical Union) vol 186 pp 293–7
- [75] Moran P A P 1948 The interpretation of statistical maps *J. R. Stat. Soc. B* **10** 243–51
- [76] Duque J C, Ramos R and Suriñach J 2007 Supervised regionalization methods: a survey *Int. Reg. Sci. Rev.* **30** 195–220
- [77] Wei R, Rey S and Knaap E 2021 Efficient regionalization for spatially explicit neighborhood delineation *Int. J. Geogr. Inf. Sci.* **35** 135–51
- [78] Garretton M and Sanchez R 2016 Identifying an optimal analysis level in multiscale regionalization: a study case of social distress in greater Santiago *Comput. Environ. Urban Syst.* **56** 14–24
- [79] Pedregosa F et al 2011 Scikit-learn: machine learning in Python *J. Mach. Learn. Res.* **12** 2825–30
- [80] Murtagh F and Legendre P 2014 Ward's hierarchical agglomerative clustering method: which algorithms implement Ward's criterion? *J. Classif.* **31** 274–95
- [81] Calinski R B and Harabasz J 1974 A dendrite method for cluster analysis *Commun. Stat. Theory Methods* **3** 1–27
- [82] Anselin L and Rey S J 2014 *Modern Spatial Econometrics in Practice. A Guide to GeoDa, GeoDaSpace and Pysal* (Chicago, IL: GeoDa Press LLC)
- [83] Rey S J, Arribas-Bel D and Wolf L J 2020 Geographic data science with PySAL and the PyData stack (available at: <https://geographicdata.science/book/intro.html>)
- [84] Negrón-Juárez R I et al 2017 Windthrow variability in central Amazonia *Atmosphere* **8** 28
- [85] Gorgens E, Motta A Z, Assis M, Nunes M H, Jackson T, Coomes D, Rosette J, Aragão L E O E C and Ometto J P 2019 The giant trees of the Amazon basin *Front. Ecol. Environ.* **17** 373–4
- [86] Cohen J, Cavalcanti I F A, Braga R H M and Neto S L 2009 Squall line in the N-NE coast of South America *Weather and Climate of Brazil* ed I F A Cavalcanti, N J Ferreira, M G A J Silva and M A F Silva Dias (Sao Paulo: Oficina de Textos) pp 75–93
- [87] Tazsarek M, Allen J T, Marchio M and Brooks H E 2021 Global climatology and trends in convective environments from ERA5 and rawinsonde data *NPJ Clim. Atmos. Sci.* **4** 35
- [88] Albrecht R I, Goodman S J, Buechler D E, Blakeslee R J and Christian H J 2016 Where are the lightning hotspots on Earth? *Bull. Am. Meteorol. Soc.* **97** 2051–68
- [89] Machado L A T et al 2018 Overview: precipitation characteristics and sensitivities to environmental conditions during GoAmazon2014/5 and ACRIDICON-CHUVA *Atmos. Chem. Phys.* **18** 6461–82
- [90] Chavez S P and Takahashi K 2017 Orographic rainfall hot spots in the Andes-Amazon transition according to the TRMM precipitation radar and *in situ* data *J. Geophys. Res.* **122** 5870–82
- [91] Espinoza Villar J C, Ronchail J, Guyot J L, Cochonneau G, Naziano F, Lavado W, De Oliveira E, Pombosa R and Vauchel P 2009 Spatio-temporal rainfall variability in the Amazon basin countries (Brazil, Peru, Bolivia, Colombia, and Ecuador) *Int. J. Climatol.* **29** 1574–94
- [92] Haghtalab N, Moore N, Heerspink B P and Hyndman D W 2020 Evaluating spatial patterns in precipitation trends across the Amazon basin driven by land cover and global scale forcings *Theor. Appl. Climatol.* **140** 411–27
- [93] Figueroa N and Nobre C 1990 Precipitation distribution over central and western tropical South America *Climanalise* **5** 36–45
- [94] Salati E and Vose P B 1984 Amazon basin: a system in equilibrium *Science* **225** 129–38
- [95] Jucker T, Bongalov B, Burslem D, Nilus R, Dalponte M, Lewis S L, Phillips O L, Qie L and Coomes D A 2018 Topography shapes the structure, composition and function of tropical forest landscapes *Ecol. Lett.* **21** 989–1000
- [96] Stephenson N L and van Mantgem P J 2005 Forest turnover rates follow global and regional patterns of productivity *Ecol. Lett.* **8** 524–31
- [97] Ter Steege H F 2003 A spatial model of tree α -diversity and tree density for the Amazon *Biodivers. Conserv.* **12** 2255–77
- [98] Muscarella R, Kolyaie S, Morton D C, Zimmerman J K and Uriarte M 2020 Effects of topography on tropical forest structure depend on climate context *J. Ecol.* **108** 145–59
- [99] Ribeiro G et al 2016 Mechanical vulnerability and resistance to snapping and uprooting for central Amazon tree species *For. Ecol. Manage.* **380** 1–10
- [100] Peterson C J, Ribeiro G H P M, Negron-Juarez R, Magnabosco Marra D, Chambers J Q, Higuchi N, Lima A and Cannon J B 2019 Critical wind speeds suggest wind could be an important disturbance agent in Amazonian forests *Forestry* **92** 444–59
- [101] Nepstad D C et al 2002 The effects of partial throughfall exclusion on canopy processes, aboveground production, and biogeochemistry of an Amazon forest *J. Geophys. Res.* **107** LBA 53-1–18
- [102] Negron-Juarez R et al 2020 Calibration, measurement, and characterization of soil moisture dynamics in a central Amazonian tropical forest *Vadose Zone J.* **19** e20070
- [103] Dos Santos L T et al 2016 Windthrows increase soil carbon stocks in a central Amazon forest *Biogeosciences* **13** 1299–308
- [104] Denslow J S 1987 Tropical rainforest gaps and tree species diversity *Annu. Rev. Ecol. Syst.* **18** 431–51
- [105] Posada J M and Schuur E A G 2011 Relationships among precipitation regime, nutrient availability, and carbon turnover in tropical rain forests *Oecologia* **165** 783–95

- [106] Taylor P G, Cleveland C C, Wieder W R, Sullivan B W, Doughty C E, Dobrowski S Z and Townsend A R 2017 Temperature and rainfall interact to control carbon cycling in tropical forests *Ecol. Lett.* **20** 779–88
- [107] Quesada C A et al 2010 Variations in chemical and physical properties of Amazon forest soils in relation to their genesis *Biogeosciences* **7** 1515–41
- [108] Martin S T et al 2017 The Green Ocean Amazon experiment (GoAmazon2014/5) observes pollution affecting gases, aerosols, clouds, and rainfall over the rain forest *Bull. Am. Meteorol. Soc.* **98** 981–97
- [109] Ter Steege H et al 2006 Continental-scale patterns of canopy tree composition and function across Amazonia *Nature* **443** 444–7
- [110] Phillips O L, Brienen R J W and Collaboration R 2017 Carbon uptake by mature Amazon forests has mitigated Amazon nations' carbon emissions *Carbon Balance Manage.* **12** 12
- [111] Harris N L et al 2021 Global maps of twenty-first century forest carbon fluxes *Nat. Clim. Change* **11** 234–40
- [112] Negrón-Juárez R I, Baker D B, Chambers J Q, Hurtt G C and Goosem S 2014 Multi-scale sensitivity of Landsat and MODIS to forest disturbance associated with tropical cyclones *Remote Sens. Environ.* **140** 679–89
- [113] Feng Y L, Negron-Juarez R I and Chambers J Q 2021 Multi-cyclone analysis and machine learning model implications of cyclone effects on forests *Int. J. Appl. Earth Obs. Geoinf.* **103** 102528
- [114] Bradstock R A, Hammill K A, Collins L and Price O 2010 Effects of weather, fuel and terrain on fire severity in topographically diverse landscapes of south-eastern Australia *Landsc. Ecol.* **25** 607–19
- [115] Buma B and Johnson A C 2015 The role of windstorm exposure and yellow cedar decline on landslide susceptibility in southeast Alaskan temperate rainforests *Geomorphology* **228** 504–11